J Geophys (1987) 61:110–121

Journal of Geophysics

Two-dimensional modelling of a towed transient magnetic dipole-dipole sea floor EM system

R.N. Edwards [1] * **and S.J. Cheesman** [2]

[1] Institute of Geophysics and Planetary Physics, Scripps Institution of Oceanography, University of California at San Diego, La Jolla, Ca., USA, 92093

[2] Department of Physics, University of Toronto, Toronto, Ontario, Canada, M5S 1A7

Abstract. The discovery of massive sulphide deposits along mid-ocean ridges has prompted the development of towed sea floor electromagnetic mapping tools. One suitable configuration of transmitter and receiver is the in-line, coaxial, magnetic dipole-dipole. The step response of this system to a double half-space model has two distinct parts. The position in time of the initial event is indicative of the conductivity of the sea floor. A reduction in dimensionality greatly simplifies the analytic and numerical computation of more complicated cases. The transmitter is reduced to a pair of horizontal line sources carrying equal but opposite currents and separated by a small vertical distance. The transient responses of the simplified system and the coaxial system to the double half-space model are remarkably similar, even though the electromagnetic mode characterised by vertical current flow is excluded by the simplification. The analytic form of the sensitivity function enables a simple expression for a depth of investigation beneath the sea floor to be derived as a function of time. The magnetic effects of currents impressed in a two-dimensional conductive target embedded in the sea floor by a horizontal magnetic point dipole transmitter may be represented approximately by a system of vortex currents only. Since vortex current flow is the type of current flow induced in a two-dimensional target by a two-dimensional magnetic source, the principal characteristics of the three-dimensional problem can be studied by two-dimensional modelling. The scattered fields from a thin conductive dike and a thin conductive sill are evaluated by setting up and solving a boundary element integral equation in the electric field. Transient response curves are presented for a limited range of models. The sea floor conductivity is fixed at 1/30 that of seawater, a typical value for recent basalt. The array size and plate depth extent are fixed at 100 m and 25 m, respectively, while the depth of burial is allowed to vary from 4 m to 25 m. The ratio of the inductive response parameter of the plate to the response parameter of the crust, which determines the degree of influence of the plate conductor on the combined step response, is varied from 0.4 to 10. Increasing the relative effect of the target delays the onset and decreases the gradient of the initial part of the response. Pronounced minima in the response as a function of array location are observed when either the transmitter or the receiver cross over the target. The minimum field over a wide range of times is close to zero for a shallow dike due to the combined shielding effect of the dike and the seawater. The shallow dike may be distinguished from a shallow sill by the shape of the minima.

Key words: Offshore, EM, Exploration

* *On leave from:* Department of Physics, University of Toronto, Toronto, Ontario, Canada, M5S 1A7

Offprint requests to: R.N. Edwards

Introduction

The report by Francheteau et al. (1979), of the discovery of massive sulphide deposits and high-temperature hydrothermal vents on the East Pacific Rise, spurred an international effort to investigate similar phenomena at other sites of sea floor spreading along the 60000 km mid-ocean ridge system and opened the possiblity of deep sea mining. Sulphide mineralisation relatively rich in gold, silver, copper, zinc and manganese has since been mapped on the crest of the East Pacific Rise (Hekinian et al., 1980), on the Galapagos Ridge (Malahoff, 1982), on the Juan de Fuca plate (Normark et al., 1983; Koski et al., 1985; Tivey and Delaney, 1985) and elsewhere on the world-wide ridge system (Rona, 1985). The deposits were initially located visually with submersibles. Some have been mapped acoustically with instrument packages like SEABEAM (Ballard and Francheteau, 1982), which are capable of determining the depth with high resolution. While these methods have been able to examine surficial geology, they are incapable of adequately assessing the extent of the deposits and the structure of the region in which they are found. Sea floor conductivity mapping using the electromagnetic method is one of the few geophysical tools suitable for this purpose.

Over the continents, electromagnetic mapping is routinely carried out by air. A simple apparent-resistivity map, often produced on-line from the output of a towed airborne EM system, has proven capable of discriminating between different types of rock and directly identifying local three-dimensional targets such as base metal mineral deposits. The latter have the property of being much more conductive than the host rocks in which they are found. It is our aim to produce a similar mapping tool for the sea floor operating on a similar scale, on the order of a hundred metres.

To be useful, any deep-towed EM system must be sensitive to the electrical conductivity of the sea floor. The conductivity of the sea floor is usually much less than that

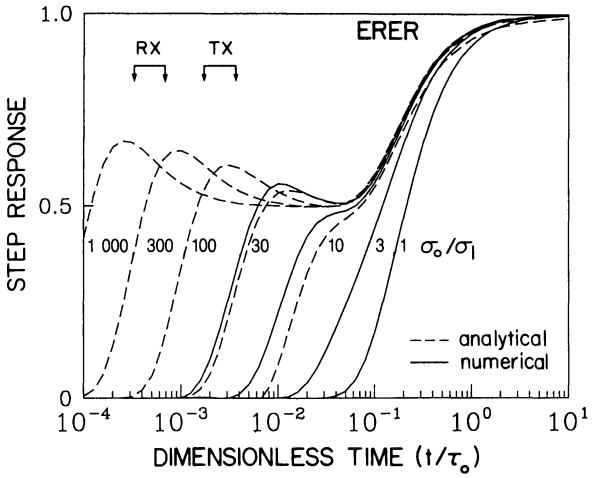

Fig. 1. The step-on response of the double half-space model to the coaxial electric dipole-dipole system (after Cheesman et al. 1987)

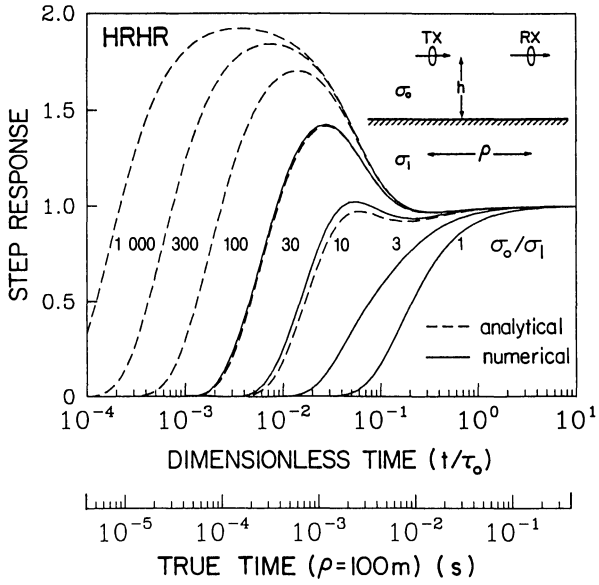

Fig. 2. The step-on response of the double half-space model to the coaxial magnetic dipole-dipole system (after Cheesman et al. 1987). The second time axis gives the true response time for a sea floor system in which the conductivity σ_0 and separation ρ are 3 S/m and 100 m, respectively

of the seawater above it. Electromagnetic fields diagnostic of sea floor conductivity have to be measured at or near the surface of what behaves as a nearly perfect conductor, at the relevant operational frequencies or delay times. The consequence of this is that some EM systems, commonly used for continental surveys, are unsuitable for sea floor conductivity assessment. The horizontal coplanar coil system, popularly called Slingram, comes to mind. The receiver measures the component of the magnetic field normal to the sea floor, which is very small for the band of frequencies of interest.

The wide range of conductivities expected for the sea floor, combined with the even wider range of anticipated electromagnetic response numbers for an embedded target, dictate the use of a broad-band EM system. Most modern receivers detect the transient fields caused by currents induced in the ground by a distinct event, such as the rapid turn-off of a constant current in the transmitter. The transient system is preferred over a continuous-wave switched-frequency system for many reasons including electronic simplicity, the absence of a response due to surficial conductors at late time and the measurement of a purely secondary signal. The last reason is not valid for a sea floor system because there is nothing equivalent to an air-wave at the receiver. The point is best illustrated by example. Edwards and Chave (1986) computed the response of a crustal half-space beneath a more conductive half-space representing seawater to a transient in-line electric dipole-dipole system. The electromagnetic field excited by an event in the transmitter diffuses outwards from it through both the seawater and the relatively less conductive sea floor. The rate of diffusion through a medium is inversely proportional to the conductivity of the medium, so that in the most common instance of a resistive sea bed, the electromagnetic field diffusing through the sea floor reaches the receiver first. At later times the signal diffusing through the seawater arrives, and ultimately the measured field approaches the static limit. Edwards and Chave (1986) showed that the transient coaxial electric dipole-dipole system is particularly useful for determining sea floor conductivity. The normalized step-on response of this system is plotted in Fig. 1 for a range of values of the conductivity ratio between the seawater and the sea floor as a function of dimensionless time, which is true time divided by the constant τ_0, the characteristic diffusion time for electromagnetic signals in seawater (see expression 25). The initial step to just over half the static limit is due to propagation in the sea floor; the second step at constant later time is due to propagation in the sea. Clearly, the position in time of the initial rise in the sea floor response is a direct measure of the sea floor conductivity and, for many practical values of the conductivity ratio, the separation in time between the two parts of the transient response, and hence the resolution of sea floor conductivity, is substantial.

Cheesman et al. (1987) addressed the obvious question: "What other transient electromagnetic systems show similar characteristics when operated in the marine environment?" They evaluated the responses of a wide variety of systems at the boundary of two half-spaces. The diagnostic separation in time between two parts of the transient response does not occur for many other systems. A change in conductivity of the sea floor produces a second-order perturbation in what is essentially a seawater response. Only the horizontal, coaxial, magnetic dipole-dipole system was added to the list of suitable geometries. The normalised step-on response of this system is plotted in Fig. 2 for a range of values of the conductivity ratio between the seawater and the sea floor. Clearly, Figs. 1 and 2 resemble one another. The tendency of the magnetic field at early time to rise to twice the free-space field following the decay of induced currents in the crust can be understood in terms of a Maxwell image of the transmitter in the conductive ocean.

From a practical point of view, the coaxial magnetic system can be constructed as a sea floor towed array, so that it deserved further study. The step-on response to several other simple geological models – the resistive layer, the resistive and conductive basement, and the vertical conductive dike – selected to illustrate salient physics, were documented and estimates of two possible sources of error asso-

ciated with the use of a practical system were obtained. Errors due to imperfect positioning were estimated by raising the receiver off the sea floor, while those due to misalignment of the transmitter were estimated by determining the radial magnetic field produced by a vertical transient magnetic dipole transmitter.

Cheesman et al. (1987) point out that preconceptions based on the use of the system on land can be quite misleading when sea floor responses have to be estimated. The fact that a thin resistive zone responds at all is a case in point. The horizontal coaxial system, indeed any system with a magnetic source, generates only horizontal current flow in a layered ground when operated at the free land-air surface. It is virtually insensitive to an intermediate, horizontal resistive zone because little current is induced in the zone. On the sea floor, the same system induces both horizontal and vertical current flow in a layered earth, and the resistive zone is detected by virtue of its pronounced effect on the latter.

Cheesman et al. (1987) also computed the response of the system to a semi-infinite vertical dike embedded in the sea floor. If the transmitter and receiver straddle the dike, the effect of the dike is to delay the initial part of the transient response. The delay as an increment from that caused by the crustal half-space alone varies linearly with dike conductance. This suggested that time delay could be inverted directly to give some measure of the anomalous integrated conductivity of the sea floor which lies both between and in the vicinity of the transmitter and receiver. It is this observation that deserves further study for, if generally applicable, it could open the way for a tomographic reconstruction of conductivity anomalies from multiple profiles over the sea floor.

Two-dimensional modelling

The purpose of the current paper is to illustrate further some of the characteristics of the EM response of the sea floor to a towed magnetic dipole-dipole system. A reduction in the dimensionality of the problem greatly simplifies both analytic and numerical computation. The point dipole is integrated along a defined strike to yield a two-dimensional source; a pair of horizontal wires carrying equal but opposite currents and separated by a small vertical distance. We show that the response of the double half-space model to this source is similar to the response of the same model to the point dipole source, even though one of the two modes of current flow described above is absent. Vertical current flow cannot be induced by a long wire magnetic source in any two-dimensional model.

The theory of EM induction by a single line source in a conductive layered medium was set out by Wait (1953), and it has been extended by many other researchers. Inan et al. (1986) have compiled an up-to-date survey of the available literature. The earlier work is adapted for a dipolar source, and closed form expressions for the general layered-earth response are derived both in the frequency and time domains. The expressions are reduced to very simple analytical forms for the special model of two half-spaces in contact. Sensitivity functions for the double half-space problem are also obtained in the time domain.

The anomalous electric current flow associated with a two-dimensional conductive inhomogeneity in a host medium excited by a horizontal point magnetic dipole is of two distinct forms: a channelled current exchange between the inhomogeneity and the host, limited by the build up of charge on the inhomogeneity, and a vortex current flow confined to the inhomogeneity whose magnetic field opposes the local rate of change of magnetic flux. The limitations in representing the three-dimensional problem by a two-dimensional approximation which cannot represent the current gathering effect are reasonably well understood and can be found in the literature, provided the target is buried in a single conductive half-space. For a double half-space host medium, there is no equivalent pool of knowledge. Further, in our problem, there is one obvious *channelling* mode which forms a very significant part of the total anomalous current flow, for targets which outcrop (or come close to it). It is a current flow in a vertical plane from the sea, through the target and back to the sea. Cheesman et al. (1987) have shown using image theory that the mode produces the same *magnetic* field at the receiver as a *vortex* circulating entirely within a composite conductor formed of the target and its image in the sea layer. Consequently, a study of the interaction of a two-dimensional target with the two-dimensional source can reveal the principal characteristics of this three-dimensional problem. We have selected two kinds of targets: the thin conductive dike and the thin conductive sill. The scattered fields are evaluated by setting up and solving a boundary element integral equation in the electric field.

Theory

The forward layered-earth problem

The problem is solved in cartesian coordinates with the y-axis along strike. The plane $z=0$ represents the sea floor, and z increases downwards. The sea is represented by an upper half-space of uniform conductivity σ_0. The conductivity $\sigma(z)$ of the crustal rock beneath the sea is isotropic and varies only in the vertical direction. The source consists of two long, horizontal wires, located in the sea at $x=0$, $z=z_0$ and $x=0$, $z=z_0+\Delta$, carrying currents of strength $+I(t)$ and $-I(t)$, respectively. The moment $M(t)$ of the linear dipole produced is defined as $I(t)\,\Delta$.

Let $M(t)$ vary as $M\exp(i\omega t)$. The problem is two-dimensional in the space variables x and z; current flow is only in the y direction and is symmetric in x. The electric field vector $\mathbf{E}$ is

$$\mathbf{E}=E(x,z,\omega)\exp(i\omega t)\,\hat{y}, \tag{1}$$

where $E(x,z,\omega)$ is the inverse cosine transform of a kernel function $E(\lambda,z,\omega)$ defined as

$$E(x,z,\omega)=\int_0^\infty E(\lambda,z,\omega)\cos(\lambda x)\,d\lambda. \tag{2}$$

The magnetic field has two components in the vertical and across-strike directions, related to the single along-strike component of the electric field by Faraday's law. Expressions for the electric and acros-strike magnetic field kernels on the sea floor may be found by integrating the corresponding fields of point dipoles distributed uniformly along strike. The latter are usually expressed in terms of Hankel

transforms (Cheesman et al. 1987; Chave and Cox, 1982) and are, in general, made up of two parts, corresponding with the two independent toroidal and poloidal modes of propagation. The modes are characterised by the absence of a vertical magnetic and vertical electric field component respectively. Only the poloidal forms can exist in the model considered here. Integrals of the Sonine-Gegenbauer type (Luke, 1962) simplify the resulting double integrals. There results

$$E(\lambda, 0, \omega) = \frac{i\omega\mu M}{2\pi} \frac{2\theta_0 Q(0) \exp(-\theta_0 |z_0|)}{1+\theta_0 Q(0)} \tag{3}$$

and

$$B_x(\lambda, 0, \omega) = -\frac{\mu M}{2\pi} \frac{2\theta_0 \exp(-\theta_0 |z_0|)}{1+\theta_0 Q(0)}, \tag{4}$$

where the wavenumber θ_0 and the parameter $Q(z)$ are given by

$$\theta_0^2 = \lambda^2 + \alpha_0^2 = \lambda^2 + i\omega\mu\sigma_0 \tag{5}$$

and

$$Q(z) = -E(\lambda, z, \omega)/i\omega B_x(\lambda, z, \omega) = -E(\lambda, z, \omega)/E'(\lambda, z, \omega), \tag{6}$$

respectively, and the prime denotes differentiation with respect to z. The parameter $Q(z)$ is continuous across all horizontal planes in the model which do not contain the source. If the crustal zone happens to be plane layered, it is possible to find $Q(0)$ given the conductivities and thicknesses of crustal layers only, by means of a recurrence rule (Wait, 1962). The value of $Q(0)$ is then substituted into expressions (3) or (4) and the fields evaluated through the inverse cosine transform (2).

The sensitivity function

The measured magnetic component $B_x(x, 0, \omega)$ on the sea floor changes when any small change $\delta\sigma$ occurs in the sea floor conductivity $\sigma(z)$ over an interval δz at some depth z. The total change in the magnetic component is related to systematic small changes in the resistivity at all depths by the integral

$$\delta B_x(x, 0, \omega) = \int_0^\infty F(\log\sigma, x, z, \omega)\, \delta(\log\sigma)\, dz, \tag{7}$$

where $\delta(\log\sigma)$ is the fractional change in conductivity at depth z. The function F is the sensitivity function or Frechet kernel. Our aim is to determine an expression for the sensitivity function for the general 1-D model, initially in $[\lambda, \omega]$-space. The expression is evaluated subsequently, explicitly for given values of x for specific simple models. The shapes of the resulting functions are analysed to obtain the penetration depths and the resolution depth intervals associated with a given model and given measurements, both in time and frequency.

Parker (1977), Fullagar and Oldenburg (1984) and Chave (1984) have shown that a sensitivity integral for the parameter Q may be written as

$$\delta Q(\lambda, 0, \omega) = -\int_0^\infty \frac{\alpha^2(z)\, E^2(z)}{E'^2(0)}\, \delta \log[\sigma(z)]\, dz. \tag{8}$$

The perturbation $\delta B_x(0)$ remains to be found. It is related to $\delta Q(0)$ by the rule

$$\delta B_x(0) = \frac{\partial B_x(0)}{\partial Q(0)}\, \delta Q(0). \tag{9}$$

The derivative of expression (4) combined with expression (9) yields

$$\delta B_x(\lambda, 0, \omega) = -\frac{\mu M}{2\pi} \frac{2\theta_0^2 \exp(-\theta_0 |z_0|)}{[1+\theta_0 Q(0)]^2} \cdot \int_0^\infty \frac{\alpha^2(z)\, E^2(z)}{E'^2(0)}\, \delta \log[\sigma(z)]\, dz, \tag{10}$$

and, by inspection, the required sensitivity function is

$$F(\log\sigma, \lambda, z, \omega) = -\frac{\mu M}{2\pi} \frac{2\theta_0^2 \exp(-\theta_0 |z_0|)}{[1+\theta_0 Q(0)]^2} \frac{\alpha^2(z)\, E^2(z)}{E'^2(0)}. \tag{11}$$

Analytical solutions for the case of a uniform half-space

If the crustal zone has uniform conductivity σ_1, the fields decay exponentially with increasing z and are porportional to $\exp(-\theta_1 z)$. The value of $Q(z)$ is therefore constant everywhere and given by

$$Q(z) = 1/\theta_1. \tag{12}$$

The form of the magnetic component B_x for the model of a uniform crustal layer beneath the sea may now be obtained by setting this value for $Q(0)$ in (4). It is

$$B_x(\lambda, 0, \omega) = -\frac{\mu M}{2\pi} \frac{2\theta_0\theta_1 \exp(-\theta_0 |z_0|)}{\theta_0+\theta_1}, \tag{13}$$

and the corresponding component in $[x, \omega]$-space is the inverse cosine transform defined by expression (2) as

$$B_x(x, 0, \omega) = -\frac{\mu M}{2\pi} \int_0^\infty \frac{2\theta_0\theta_1 \exp(-\theta_0 |z_0|)}{\theta_0+\theta_1} \cos(\lambda x)\, d\lambda. \tag{14}$$

At zero frequency, the expression simplifies to

$$B_x^{DC}(x, 0, \omega) = -(\mu M/2\pi) \int_0^\infty \lambda \exp(-\lambda |z_0|) \cos(\lambda x)\, d\lambda. \tag{15}$$

which has the well-known form

$$B_x^{DC}(x, 0, \omega) = (\mu M/2\pi) \frac{(x^2 - z_0^2)}{(x^2+z_0^2)^2}, \tag{16}$$

and which reduces, in turn, to $\mu M/2\pi x^2$ for vanishing z_0.

If the transmitter and receiver both lie on the sea floor, then expression (14) takes on a form which is invariant under an exchange of half-space indices. The integral may be normalised for convenience by dividing by the zero-frequency response. The result is

$$B_x^n(x, 0, \omega) = -x^2 \int_0^\infty \frac{2\theta_0\theta_1}{\theta_0+\theta_1} \cos(\lambda x)\, d\lambda. \tag{17}$$

The integral may be rearranged as

$$B_x^n(x,0,\omega)=\frac{2x^2}{i\omega\mu(\sigma_0-\sigma_1)}\cdot\int_0^\infty[(\lambda^2+\alpha_1^2)\theta_0-(\lambda^2+\alpha_0^2)\theta_1]\cos(\lambda x)\,d\lambda. \quad (18)$$

Two types of integrals need to be evaluated. The first is of the form

$$\lim_{h\to 0}\int_0^\infty \theta\exp(-\theta h)\cos(\lambda x)\,d\lambda$$

$$=-\lim_{h\to 0}\frac{\partial}{\partial h}\int_0^\infty \exp(-\theta h)\cos(\lambda x)\,d\lambda \quad (19)$$

$$=-\lim_{h\to 0}\frac{\partial}{\partial h}\left[\frac{\alpha h}{(x^2+h^2)^{1/2}}K_1\{\alpha(x^2+h^2)^{1/2}\}\right], \quad (20)$$

by formula 1.4.26 of Erdelyi et al. (1954),

$$=-\alpha K_1(\alpha x)/x. \quad (21)$$

The second integral is a double derivative of the first with respect to x, and is given by

$$\lim_{h\to 0}\int_0^\infty \lambda^2\theta\exp(-\theta h)\cos(\lambda x)\,d\lambda$$

$$=\frac{6\alpha}{x^3}K_1(\alpha x)+\frac{\alpha^3}{x}K_1(\alpha x)+\frac{3\alpha^2}{x^2}K_0(\alpha x). \quad (22)$$

The final normalised form of the frequency-domain solution is

$$B_x^n(x,0,\omega)=\frac{2}{\sigma_0-\sigma_1}\left[\left\{(\sigma_0-\sigma_1)\alpha_0 x+\frac{6\sigma_0}{\alpha_0 x}\right\}K_1(\alpha_0 x)+3\sigma_0 K_0(\alpha_0 x)\right]$$

$$+\text{the above with the subscripts on } \alpha \text{ and } \sigma \text{ exchanged.} \quad (23)$$

Assuming zero initial conditions, the Laplace transform of the magnetic component $B_x(x,0,s)$ is the un-normalised version of (23) with the product $i\omega$ replaced by the Laplace variable s. It is

$$B_x(x,0,s)=\frac{\mu M(s)}{(\sigma_0-\sigma_1)\pi x^2}\cdot\left[\left\{(\sigma_0-\sigma_1)\sqrt{\tau_0 s}+\frac{6\sigma_0}{\sqrt{\tau_0 s}}\right\}K_1(\sqrt{\tau_0 s})+3\sigma_0 K_0(\sqrt{\tau_0 s})\right]$$

$$+\text{the above with the subscripts on } \tau \text{ and } \sigma \text{ exchanged,} \quad (24)$$

where the electromagnetic diffusion time constant for the ith medium is

$$\tau_i=x^2\mu\sigma_i. \quad (25)$$

Expression (24) may be inverted to the time domain if the Laplace transform of the source dipole moment $M(s)$ is specified. A current I switched on at time $t=0$ for a time dt has the constant transform Mdt and the corresponding impulse response may be obtained from standard tables of Laplace transforms as

$$dB_x^I(x,0,t)=\frac{\mu M dt}{(\sigma_0-\sigma_1)\pi x^2 t}\cdot\left[\left\{(\sigma_0-\sigma_1)+\frac{6\sigma_0 t}{\tau_0}\right\}\left\{\frac{\tau_0}{4t}\right\}+\frac{6\sigma_0 t}{\tau_0}\right]\exp(-\tau_0/4t)$$

$$+\text{the above with the subscripts on } \tau \text{ and } \sigma \text{ exchanged.} \quad (26)$$

If the current I in the dipole is switched on at time zero and held on indefinitely, then the step response $B_x^S(x,0,t)$ obtained is the integral

$$B_x^S(x,0,t)=\int_0^t dB_x^I(x,0,t). \quad (27)$$

The integral may be evaluated by inspection, and the resulting field may be normalised by the low-frequency or, equivalently, the late-time value defined in expression (16). There results

$$B_x^{Sn}(x,0,t)=\frac{2}{\sigma_0-\sigma_1}\left[(\sigma_0-\sigma_1)+\frac{6\sigma_0 t}{\tau_0}\right]\exp(-\tau_0/4t)$$

$$+\text{the above with the subscripts on } \tau \text{ and } \sigma \text{ exchanged.} \quad (28)$$

In the lower half-space the ratio of the electric field to its vertical derivative may be written as

$$E_1(\lambda,z)/E_1'(\lambda,0)=-\exp(-\theta_1 z)/\theta_1. \quad (29)$$

Hence, the half-space sensitivity functions in $[\lambda,\omega]$-space and $[x,\omega]$-space, respectively, are

$$F(\log\sigma_1,\lambda,z,\omega)=-\frac{\mu M}{2\pi}\frac{2\theta_0^2\alpha_1^2(z)\exp(-2\theta_1 z)}{(\theta_0+\theta_1)^2} \quad (30)$$

and

$$F(\log\sigma_1,x,z,\omega)=-\frac{\mu M}{2\pi}\cdot\int_0^\infty\frac{2\theta_0^2\alpha_1^2(z)\exp(-2\theta_1 z)}{(\theta_0+\theta_1)^2}\cos(\lambda x)\,d\lambda. \quad (31)$$

The actual change observed in the magnetic field at the receiver when a small fractional change $\delta\log(\sigma_1)$ occurs over a small interval δz about the depth z in the half-space is the product of expression (31) with $\delta\log(\sigma_1)\,\delta z$, by definition. The cosine transform can only be evaluated analytically for the special case of a perfectly conductive sea layer. Then

$$F(\log\sigma_1,x,z,\omega)=-\frac{\mu M}{2\pi}\int_0^\infty 2\alpha_1^2\exp(-2\theta_1 z)\cos(\lambda x)\,d\lambda$$

$$=-\frac{4\mu M\alpha_1^3 z}{2\pi(x^2+4z^2)^{1/2}}K_1\{\alpha_1(x^2+4z^2)^{1/2}\}. \quad (32)$$

Expressions for the sensitivity function in the time domain for impulsive and step sources are obtained in the manner described earlier for computing transient magnetic fields from their frequency response. In expression (31), product $i\omega$ is replaced by the Laplace variable s and appropriate forms are inserted for the moment $M(s)$. The evaluation of the transient sensitivity functions $F^I(\log\sigma_1, x, z, t)$ and $F^S(\log\sigma_1, x, z, t)$ requires in general both a numerical inverse cosine transform and a numerical inverse Laplace transform. The Laplace transform of the kernel function is performed under the cosine integral, using the Gaver-Stehfest algorithm described in the Appendix. The kernel has to be evaluated for a set of eight real values of the Laplace variable s for wavenumbers λ specified by the inverse cosine transform algorithm. The latter is a variation of the inverse Hankel transform described by Chave (1983), modified for half-integer-order Bessel functions. The special case of a perfectly conductive sea layer over a crustal half-space leads to an analytical form. For example, if the constant amplitude source moment M in (32) is replaced by a weighted $M(s)$ of M/s, then the step sensitivity function may be evaluated using standard tables as

$$F^S(\log\sigma_1, x, z, t)=\frac{\mu M}{2\pi}\frac{z(\mu\sigma_1)^2}{t^2}\exp\{-\mu\sigma_1(x^2+4z^2)/4t\}. \tag{33}$$

The anomalous effect of a thin dike

A two-dimensional vertical plate, width a, conductivity-thickness product S, is located at a depth d below the sea floor in crustal material of constant conductivity σ_1, as shown in Fig. 3. It is excited by the horizontal, long-wire dipole which is a horizontal distance x_t away. The moment $M\exp(i\omega t)\,\hat{x}$ of the dipole is as defined previously. The receiver which measures the x-component of the magnetic field on the sea floor is at a distance x_r from the plate.

The plate is divided up into infinitesimal strips of width $d\zeta$. Let the induced secondary surface current on a given strip be $K(\zeta)$. It is the *total* integrated current density through the plane of the plate, because the plate has infinitesimal thickness, so that the contribution from the primary current flow is itself infinitesimal. It follows that the total electric field within the strip is $K(\zeta)/S$. An integral equation can be formed by equating this internal tangential electric field to the corresponding external electric field at the surface of the strip. The latter is simply expressed as a sum of the external field of the plate current distribution and the field of the exciting dipole source.

Let $P(z)$ be a test point on the surface of the plate. The external electric field $dE^s(z)$ at P due to a strip of current at ζ is

$$dE^s(z)=-\frac{i\omega\mu K(\zeta)\,d\zeta}{2\pi}\left[K_0\{\alpha_1|z-\zeta|\}-\int_0^\infty\frac{\theta_1-\theta_0}{\theta_1(\theta_1+\theta_0)}\exp\{-\theta_1(z+\zeta)\}\,d\lambda\right], \tag{34}$$

where the form of the Green's function is given by Inan et al. (1986). The field of all such rings is

$$E^s(z)=-(i\omega\mu/2\pi)\int_d^{a+d}K(\zeta)\,d\zeta\left[K_0\{\alpha_1|z-\zeta|\}-\int_0^\infty\frac{\theta_1-\theta_0}{\theta_1(\theta_1+\theta_0)}\exp\{-\theta_1(z+\zeta)\}\,d\lambda\right]. \tag{35}$$

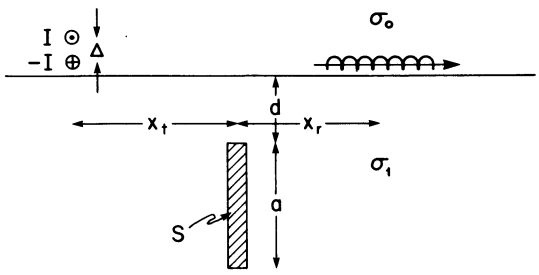

Fig. 3. The interaction of the magnetic dipole-dipole system with a vertical plate: definition of parameters

The external electric field at the point $P(z)$ due to the source magnetic dipole is

$$E^p(z)=(i\omega\mu M/2\pi)\int_0^\infty\frac{2\theta_0}{\theta_1+\theta_0}\exp(-\theta_1 z)\cos(\lambda x_t)\,d\lambda. \tag{36}$$

The total external field is the sum of the fields given in (35) and (36).

The integral equation can now be formed by equating the internal and external tangential components of the electric field at P. It is

$$K(z)/S=E^p(z)+E^s(z). \tag{37}$$

The equation may be solved numerically by the method of subsections – the boundary element technique. The strip is divided into N strips of finite thickness Δ equal to a/N. The depth to the centre of the ith ring is z_i. The integral equation in discrete form for a set of N test points z_j is

$$K(z_j)/S=E^p(x_t, z_j)+\sum_{i=1}^{N}K(z_i)\,G(i,j), \tag{38}$$

where the interaction function $G(i,j)$ is given by

$$G(i,j)=-(i\omega\mu/2\pi)\left[\int_{z_i-\Delta/2}^{z_i+\Delta/2}K_0\{\alpha_1|z_j-\zeta|\}\,d\zeta+\Delta\int_0^\infty\frac{\theta_1-\theta_0}{\theta_1(\theta_1+\theta_0)}\exp\{-\theta_1(z_j+z_i)\}\,d\lambda\right]. \tag{39}$$

For the special case $i=j$, the first term in expression (39) is evaluated analytically using the small argument form of the modified Bessel function. There results

$$\int_{z_i-\Delta/2}^{z_i+\Delta/2}K_0\{\alpha_1|z_i-\zeta|\}\,d\zeta\approx\Delta\{1-\gamma-\log(\alpha_1\Delta/4)\}, \tag{40}$$

where γ is Euler's constant. For all other cases a three-point Simpson's rule approximation to the integral suffices. The second term in expression (39) represents the correction that has to be made to a whole-space interaction function to account for the sea layer above the crustal layer. The reasonable approximation used in its evaluation is the assumption that the strip current is concentrated into a line source at its centre.

The computation of the anomalous magnetic component at the receiver point is a summation over the strip currents. For receiver points not too close to the strip, the line current approximation may again be used. There results

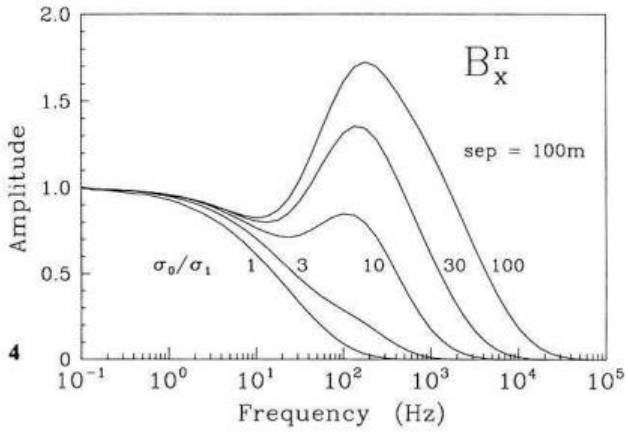

4

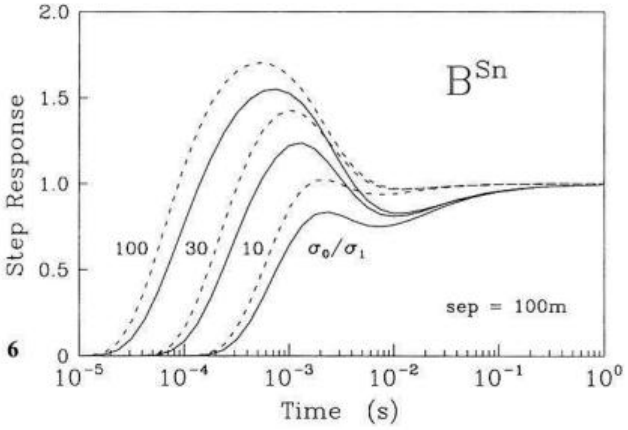

6

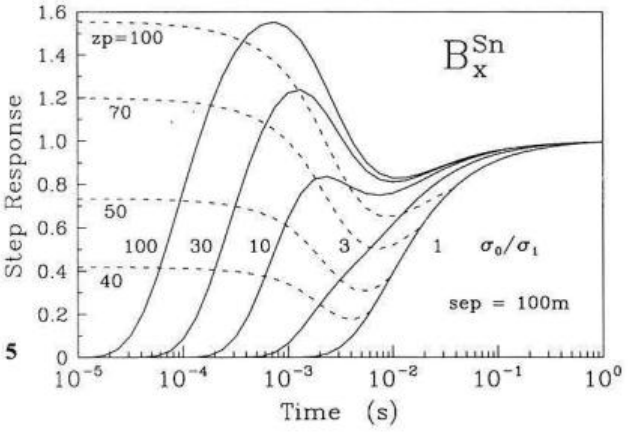

5

Fig. 4. The normalised frequency-domain amplitude response of the double half-space model to the two-dimensional dipole-dipole system computed analytically from expression (23) at a range of values of σ_0/σ_1 for σ_0 and x values of 3 S/m and 100 m, respectively

Fig. 5. The normalised transient step-on response of the double half-space model to the two-dimensional magnetic dipole-dipole system computed analytically from expression (28) for a range of values of σ_0/σ_1 and shown as *solid lines*. The loci of constant depths of investigation z_p for the same model are shown as *dashed lines*

Fig. 6. A comparison of the step-on responses of the double half-space model to the coaxial (*dashed lines*) and the two-dimensional (*solid lines*) magnetic dipole-dipole systems

$$B_x(x_r,0) = -(\mu\Delta/2\pi)\sum_{j=1}^{N} K(z_j)\int_0^{\infty}\frac{2\theta_0}{\theta_1+\theta_0}\cdot\exp(-\theta_1 z_j)\cos(\lambda x_r)\,d\lambda. \quad (41)$$

The Gaver-Stehfest algorithm may be employed to compute the transient response of the strip. The expressions given above, with $i\omega$ replaced by s and an appropriate form for the moment function $M(s)$ inserted, have to be evaluated at eight defined real values of s for every required delay time t.

Results

The double half-space response

The normalised frequency-domain amplitude response and time-domain step-on response of the two-dimensional dipole-dipole system to the double half-space model are shown in Figs. 4 and 5, respectively. The curves were computed from the analytical expressions (23) and (28), for a typical transmitter-receiver separation of 100 m and for a range of values of the conductivity ratio σ_0/σ_1. The two figures are qualitatively similar provided frequency in Fig. 4 is read as inverse time. The roll-off of the crustal response is about two and a half decades of frequency wide, while the corresponding rise in the time domain is only one and a quarter decades wide. The transient responses are compared with those of the coaxial dipole-dipole system in Fig. 6. The position in time of the initial event on both sets of curves is indicate of the conductivity of the sea floor while, at distinctly later time, a second characteristic of the transient is a measure only of the seawater conductivity. The two sets of curves are surprisingly similar, but clearly they differ in detail, following different power laws as a function of time. The nature of the differences is perhaps best understood by considering the physics of the problem, when the conductivity contrast between the sea and the sea floor is large. At early time, the sea behaves as a perfect conductor; the magnetic field observed is that of a transmitter of twice the moment in a *whole* space of conductivity σ_1 (see discussion in Cheesman et al. 1987). The whole-space conductivity model is so simple that the fundamental shape of the transient is relatively insensitive to the shape of the source. At late time, the field is that of the transmitter and the currents it induces in a half-space of conductivity σ_0. The current flow induced in the sea is horizontal and unimodal in both cases.

The set of dashed lines crossing the principal solid response curves in Fig. 5 indicate the depth of investigation of the system as a function of time for any given response. As the total field at the receiver increases, the depth of investigation of the system increases, to a maximum depth in excess of 100 m. From the point of view of physics, this behaviour is quite logical. As time progresses, the electromagnetic fields induced in the crustal half-space diffuse to greater depth and excite the deeper regions of the model. The field of the induced currents and their images in the conductive seawater, together with the constant field of the transmitter and its image in the seawater, constitute the total measured crustal response.

The definition of the depth of investigation and its deter-

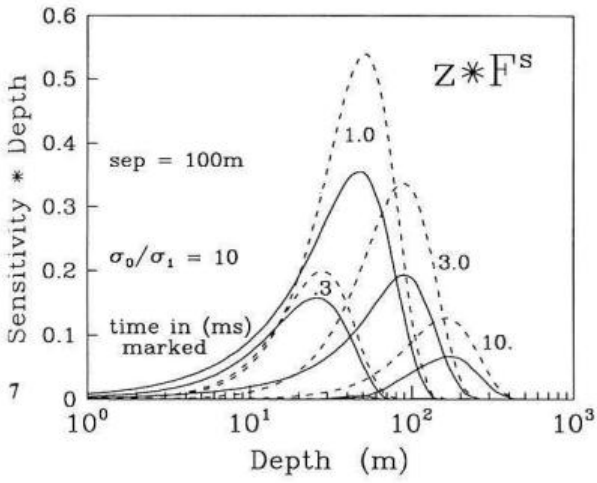

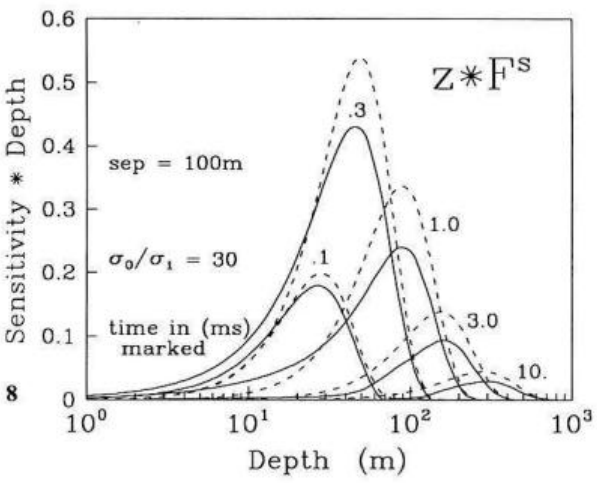

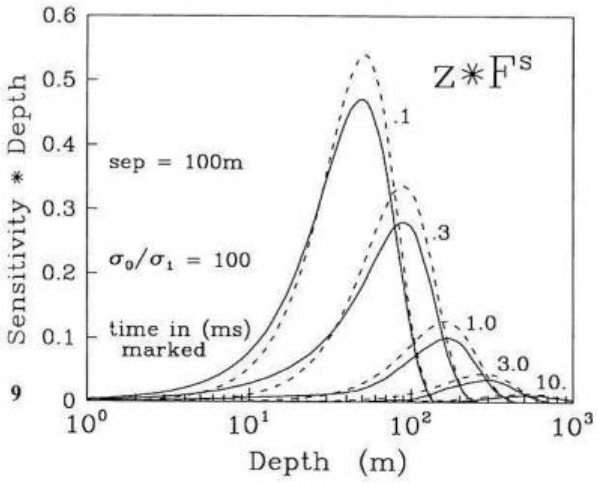

Fig. 7. The sensitivity * depth function plotted as a function of depth for several times, for σ_1 and σ_0 values of 0.3 and 3 *S*/m (*solid lines*) and 0.3 and ∞*S*/m (*dashed lines*)

Fig. 8. The sensitivity * depth function plotted as a function of depth for several times, for σ_1 and σ_0 values of 0.1 and 3 *S*/m (*solid lines*) and 0.1 and ∞*S*/m (*dashed lines*)

Fig. 9. The sensitivity * depth function plotted as a function of depth for several times, for σ_1 and σ_0 values of 0.03 and 3 *S*/m (*solid lines*) and 0.03 and ∞*S*/m (*dashed lines*)

mination as an analytic form requires a study of the transient sensitivity function. For step-on excitation the general form of the function, for arbitrary conductivity ratios, is the Laplace transform of expression (31), with source moment $M(s)$ set to M/s. The analytic reduction for a very resistive crust is given by expression (33).

The sensitivity function has the units of tesla$\cdot m^{-1}$, but a dimensionless function can be formed from it. Clearly, changes in the magnetic field can be expressed as a fraction of the free-space late-time field, by dividing the function by $\mu M/2\pi x^2$. For the shape of the sensitivity function to be useful for experimental design with this choice of a constant normalising field, the typical experimental errors expected on a measured response curve should be independent of time. The choice of a suitable scale length to multiply the function is less easy. The value chosen should be typical of the depth interval over which a conductivity change might be expected to influence the data. Intuitively, the interval should not be a constant but should increase with depth, as most users of EM systems anticipate a decrease in absolute resolution as depth increases. Consequently, the function is scaled by multiplying by the depth z. Clearly, this choice of scaling has the effect of enhancing for large z the magnitude of the sensitivity function, and the inferred depth of investigation, over a linearly scaled function. The change in the observed magnetic field at the receiver, as a fraction of the late-time field, when a small fractional change $\delta \log(\sigma_1)$ occurs over an interval z about a depth z in the half-space is the product of the final normalised sensitivity * depth function with $\delta \log(\sigma_1)$.

Normalised sensitivity * depth functions, for a range of suitable values of time, the typical transmitter-receiver separation of 100 m and a sea conductivity of 3 *S*/*m* are plotted as solid curves in Figs. 7, 8 and 9 for values of the ratio σ_0/σ_1 of 10, 30 and 100, respectively. These curves were all calculated numerically. As time increases, the EM system becomes increasingly more sensitive to the deeper zones of the half-space. As the absolute conductivity of the half-space decreases, the sensitivity function appropriate to a given depth moves to earlier time. The dashed curves on the figures, which overlie corresponding solid curves, are for the same values of the sea floor conductivity σ_1. They were evaluated from the analytic expression (33), which was derived assuming σ_0 was infinite. Qualitatively, the dashed and solid curves are similar, except for amplitude variation. In particular, the location in depth of the peaks of a solid curve and a corresponding dashed curve seem very close. The location of the peak in the dashed curve, defined here as the depth of investigation, can be found analytically. It is the value of depth z_p which maximises the product of z and the RHS of expression (33). After differentiation, the rule obtained is $z_p = \sqrt{t/\mu\sigma_1}$, and the dashed curves in Fig. 5 are simply the loci of constant z_p.

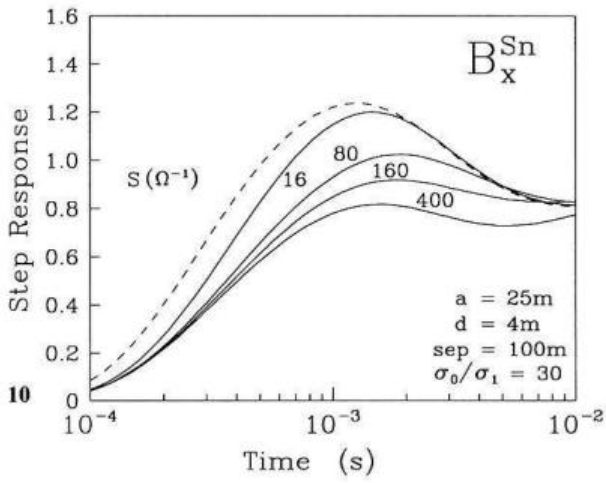

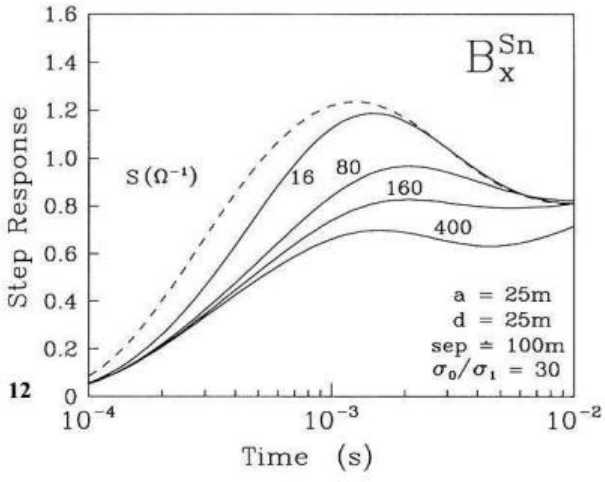

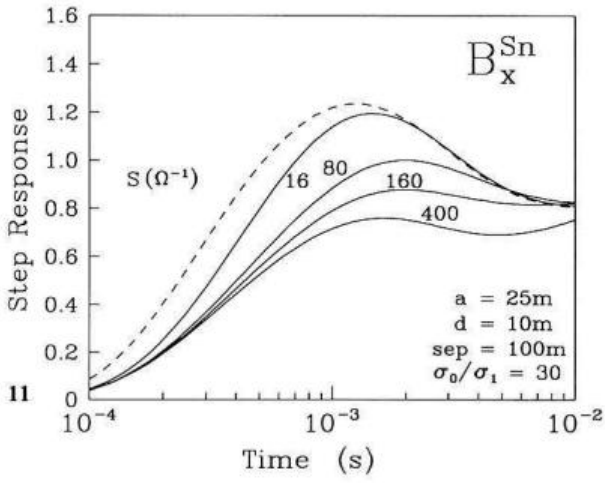

Fig. 10. The transient step-on response of the double half-space model containing a conductive vertical dike. The transmitter and receiver straddle the dike symmetrically. The depth of burial d, the conductivities σ_1 and σ_0 are 4 m, and 0.1 and 3.0 S/m, respectively

Fig. 11. The transient step-on response of the double half-space model containing a conductive vertical dike. The transmitter and receiver straddle the dike symmetrically. The depth of burial d, the conductivities σ_1 and σ_0 are 10 m, and 0.1 and 3.0 S/m, respectively

Fig. 12. The transient step-on response of the double half-space model containing a conductive vertical dike. The transmitter and receiver straddle the dike symmetrically. The depth of burial d, the conductivities σ_1 and σ_0 are 25 m, and 0.1 and 3.0 S/m, respectively

The response of the dike and the sill

The electromagnetic transient response of a finite conductor in the crustal half-space is shown with two families of curves. For the first family, the transmitter and receiver locations are fixed symmetrically about the conductor. The depth and conductivity of the anomaly are varied, and the step response is plotted as a function of time for given crustal and seawater conductivities. The curves are smooth curves and are indicative principally of the electromagnetic properties of the system. The second family of curves are designed to show the geometrical response of the anomaly. The plot is of step response against position, with time as the variable parameter. Clearly, position needs to be defined and the definition depends on how the EM system is arranged on the sea floor for successive measurements. The assumption in this work is that the transmitter-receiver combination is towed across the anomaly keeping the separation between them constant. The resulting response is symmetric about the centre of the conductor, because of the symmetry in x of the two structures studied and the symmtery of the Green's functions carrying the source field from the transmitter to the conductor and the secondary field back from the conductor to the receiver, expressions (36) and (41). The step response axis in both families of curves refers to the total step response. The secondary field due to the anomalous conductor has not been stripped from the normal, double half-space response.

The computation of results for even the geologically useful range of the many parameters would lead to an indigestible display of data. The work has to be restricted to a few typical cases illustrating the salient points of physics. Wolfgram et al. (1986) have estimated the bulk electrical conductivity of basalt in the vicinity of an active hydrothermal zone as being of the order of 0.1–0.2 S/m. Consequently, it is reasonable to fix the ratio σ_0/σ_1 at 30. The size of the ratio of the response parameter of the plate $\mu aS/t$ to the response parameter of the crust $\mu\sigma_1 x^2/t$, i.e. $aS/\sigma_1 x^2$, determines the degree of influence of the plate conductor on the combined step response. The selected set of ratios (0.4, 2.0, 4.0, 10.0) may be converted into plate conductances provided the depth extent a of the plate is specified. The choice of 25 m for a enables the effect of depth of burial d on the response curves to be quantified easily without d exceeding the transmitter-receiver separation. It follows that the set of conductances S is (16.0, 80.0, 160.0, 400.0) S.

The first family of curves for the vertical conductive plate or dike is presented in Figs. 10, 11 and 12 for values of the depth of burial of 4, 10 and 25 m, respectively. The principal effects of the dike are to delay the initial rise of the step response and to change its gradient. The frequency-domain response of an isolated conductor like a plate is approximately a single pole function which varies very rapidly with frequency, much more rapidly than the response of a distributed conductor like a half-space. As a consequence of the uncertainty principle, the step response varies

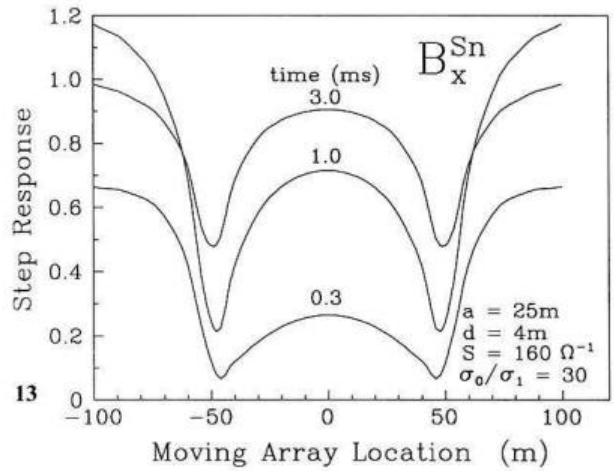

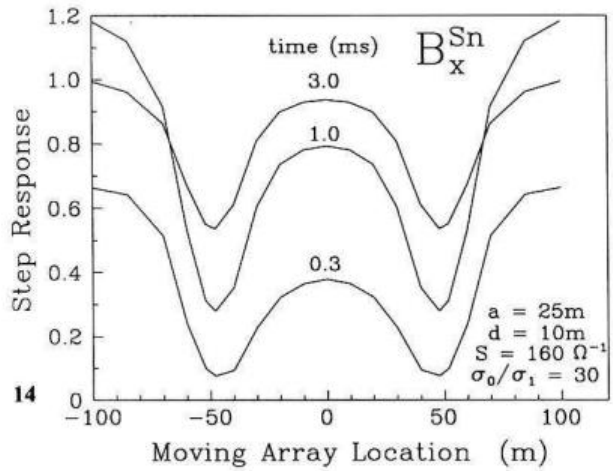

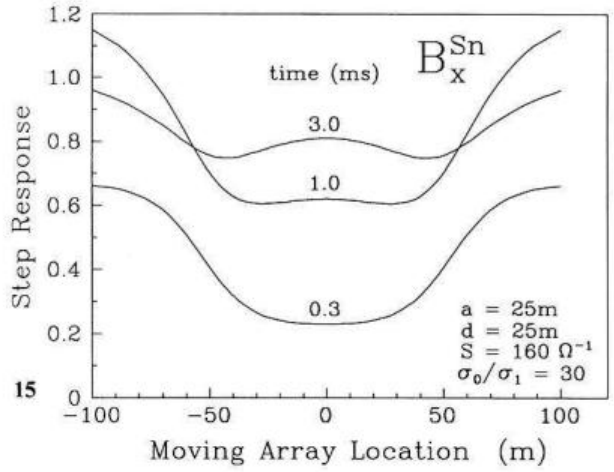

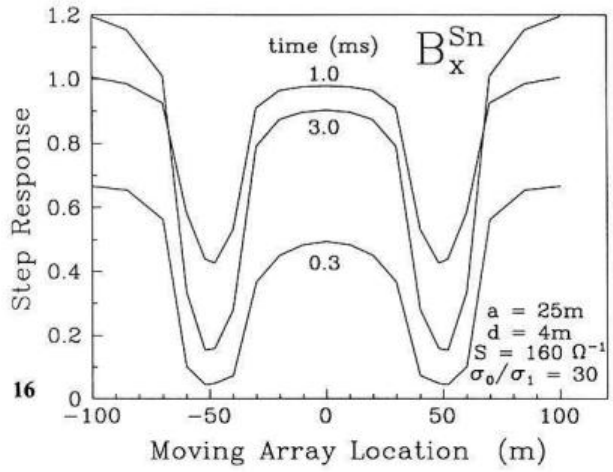

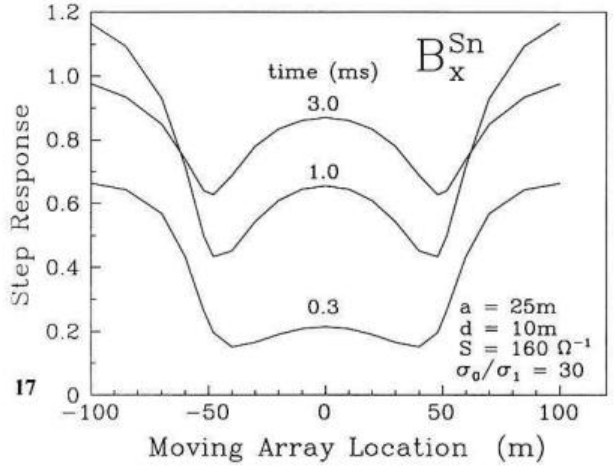

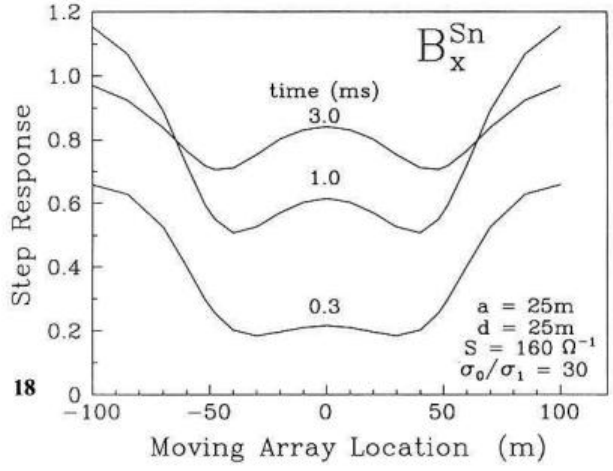

Fig. 13. The transient step-on response of the double half-space model containing a vertical dike plotted as a function of the position of a moving transmitter-receiver array for a range of times. The depth of burial of the dike d is 4 m

Fig. 14. The transient step-on response of the double half-space model containing a vertical dike plotted as a function of the position of a moving transmitter-receiver array for a range of times. The depth of burial of the dike d is 10 m

Fig. 15. The transient step-on response of the double half-space model containing a vertical dike plotted as a function of the position of a moving transmitter-receiver array for a range of times. The depth of burial of the dike d is 25 m

Fig. 16. The transient step-on response of the double half-space model containing a horizontal sill plotted as a function of the position of a moving transmitter-receiver array for a range of times. The depth of burial of the dike d is 4 m

Fig. 17. The transient step-on response of the double half-space model containing a horizontal sill plotted as a function of the position of a moving transmitter-receiver array for a range of times. The depth of burial of the dike d is 10 m

Fig. 18. The transient step-on response of the double half-space model containing a horizontal sill plotted as a function of the position of a moving transmitter-receiver array for a range of times. The depth of burial of the dike d is 25 m

as a function of time more slowly than the corresponding half-space response, which explains the change in gradient. The effect of increasing depth of burial is to increase the effect of the dike at the later times. A deeper dike is presumably better coupled to the late-time source field.

The second family of curves, the variation of the response with the position of a moving EM system, is shown in Figs. 13, 14 and 15 for the same values of depth of burial. Pronounced minima in the curves are observed when either the transmitter or the receiver are immediately above the dike. The sharpness of the minima decreases as depth of burial increases. A shallow plate has the effect of almost extinguishing the total field at the earliest times when the receiver and transmitter straddle it.

The response of a horizontal plate or sill may be computed in much the same way as the response of a dike. In fact, the software is simplified as the interaction matrix is Toeplitz no matter what the nature of the layering, and special rapid algorithms are available for inverting it. A family of curves of the second type is shown in Figs. 16, 17 and 18, for the usual set of depths of burial. The minima observed when either the transmitter or the receiver cross over the still are just as deep as but broader than the corresponding minima for the dike. The total field at early time is not as well extinguished as in the case of the dike. However, for the largest depth of burial, the responses of the dike and sill look very similar.

Conclusions

A two-dimensional problem has been studied with the aim of learning more about the physics of the response of the earth to a towed transient magnetic dipole-dipole sea floor EM system. Analytic solutions for the frequency-domain response and the step-on time-domain transient response of two half-spaces in contact have been derived. For conductivity ratios greater than about ten, the response divides into two parts. The location in time of the initial rise in the transient response provides a direct measure of the apparent conductivity of the sea floor, while the character of the signal at late times may be inverted only for seawater conductivity. Analysis of the sensitivity function for the two half-space model enables a simple expression for a depth of investigation to be derived as a function of time.

The transient responses of a dike and a sill embedded in the crustal half-space to a moving array configuration have also been examined. The added conductivity delays the rise of the initial part of the transient response as a function of time and decreases the gradient of the response. Pronounced minima in the response as a function of array location are observed when either the transmitter or the receiver cross over the target. A shallow dike may be distinguished from a shallow sill by the shape of the minima.

Appendix

Numerical inversion of the Laplace transform

Davis and Martin (1979) critically evaluated a large number of different methods for numerically inverting the Laplace transform. The Gaver-Stehfest technique is neither the most accurate nor the most generally applicable. One has to be certain *a priori* that the unknown temporal function $F(t)$ has no discontinuities, sharp peaks or rapid oscillations. However, the algorithm does offer the user the advantage of speed, simplicity and, perhaps most important of all, the need to compute the transform function $F(s)$ only for real values of the Laplace variable s. A detailed description of the algorithm may be found in Stehfest (1970) and Knight and Raiche (1982). The numerical recipe for an approximation $F_a(t)$ to the function $F(t)$ is

$$F_a(t)=\log 2/t \sum_{n=1}^{N_c} c_n F(s_n), \tag{42}$$

where the N_c discrete values of s are given by $s_n=n \log 2/t$, and the coefficients c_n by

$$c_n=(-1)^{n+N_c/2} \cdot \sum_{k=(n+1)/2}^{\min(n,N_c/2)} \frac{k^{n/2}(2k)!}{(N_c/2-k)!\,k!(k-1)!(n-k)!(2k-n)!}. \tag{43}$$

The choice of an optimum value of N_c, which must be even, depends on the precision of the machine arithmetic. Stehfest comments that, with increasing N_c, the number of correct figures in F_a first increases linearly then decreases linearly. On the IBM-PC equipped with Microsoft FORTRAN 3.1 and operating in single precision, the optimum N_c is about 8. Values of N_c significantly greater than 8 cause grossly incorrect results due to rounding error. The set of coefficients (c_n) for $N_c=8$ is

$$(-0.33333333, 48.333333, -906.00000, 5464.6667, \\ -14376.667, 18730.000, -11946.667, 2986.6667).$$

Form a purely academic point of view, it is interesting to examine the simplest Gaver-Stehfest representation, the case $N_c=2$. The set (c_1, c_2) is $(2, -2)$ and

$$F_a(t)=(2 \log 2/t)[F(\log 2/t)-F(2 \log 2/t)]. \tag{44}$$

If $F(s)$ happens to be the single pole function $1/(1+s)$, which is the principal response of a simple conductor in free space, then the approximation $F_a(t)$ and the exact inverse $\exp(-t)$ are in the ratio

(1.00, 0.70, 0.65, 0.78, 2.08, 7.84)

for values of t of

(0.0, 0.5, 1.0, 2.0, 4.0, 6.0),

respectively. The error decreases rapidly as N_c increases, and the corresponding result for $N_c=8$ is

(1.000, 0.999, 0.998, 1.007, 1.063, 0.682),

showing that the decaying exponential function could be tracked to at least one-hundreth of its original amplitude.

A more appropriate test for this project is the inverse transformation of expression (23) to the step response of the double half-space model, derived earlier analytically as expression (28). The approximate inverse transforms for values of N_c of 4, 6 and 8 are shown in Fig. 19, while the percentage error in the $N_c=8$ curve relative to the analytic inverse is shown in Fig. 20. Again, the value 8 seems adequate for N_c, as the error level over much of the time range of interest is less than 1%.

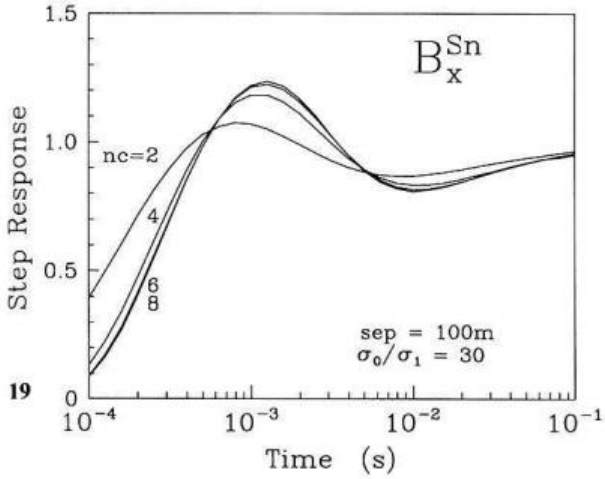

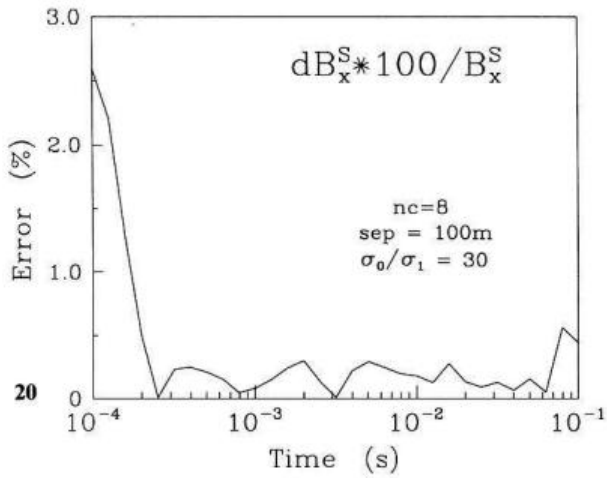

Fig. 19. The transient response computed from the frequency-domain expression (23) using the Gaver-Stehfest algorithm with different numbers of coefficients N_c. The curves converge to the analytic result given in expression (28), also shown!

Fig. 20. The percentage error in the $N_c = 8$ curve of Fig. 19 relative to the analytic solution

Acknowledgements. The sea floor transient EM project at the University of Toronto is supported by Strategic Grant # G1589 from the Natural Sciences and Engineering Research Council of Canada. The research was conducted while one of the authors (RNE) was a Cecil and Ida Green Research Foundation Scholar at the Institute of Geophysics and Planetary Physics.

References

Ballard, R.D., Francheteau, J.: The relationship between active sulphide deposition and the axial processes of the Mid-Ocean Ridge. Mar. Tech. Soc. J. **16**, 8–22, 1982

Chave, A.D.: Numerical integration of related Hankel transforms by quadrature and continued fraction expansion. Geophysics **48**, 1671–1686, 1983

Chave, A.D.: The Frechet derivatives of electromagnetic induction. J. Geophys. Res. **89**, 3373–3380, 1984

Cheesman, S.J., Edwards, R.N., Chave, A.D.: On the theory of sea floor conductivity mapping using transient EM systems. Geophysics **52**, 204–217, 1987

Davis, B., Martin, B.: Numerical inversion of the Laplace transform: a survey and comparison of methods. J. Comp. Phys. **33**, 1–32, 1979

Edwards, R.N., Chave, A.D.: On the theory of a transient electric dipole-dipole method for mapping the conductivity of the sea floor. Geophysics **51**, 984–987, 1986

Erdelyi, A., Magnus, W., Oberhettinger, F.G., Tricomi, F.G.: Tables of integral transforms **1**. New York: McGraw-Hill 1954

Francheteau, J.H., Needham, H.D., Choukroune, P., Juteau, T., Seguret, M., Ballard, R.D., Fox, P.J., Normark, W., Carranza, A., Cordoba, D., Guerrero, J., Rangin, C., Bougault, H., Cambon, P., Hekinian, R.: Massive deep-sea sulphide ore deposits discovered on the East Pacific Rise. Nature **277**, 523–528, 1979

Fullagar, P.K., Oldenburg, D.W.: Inversion of horizontal loop electromagnetic frequency soundings. Geophysics **49**, 150–164, 1984

Hekinian, R., Fevrier, M., Bischoff, J.C., Picot, P., Shanks, W.C.: Sulfur deposits from the East Pacific Rise near 21°N. Science **207**, 1433–1444, 1980

Inan, A.S., Fraser-Smith, A.C., Villard, Jr., O.G.: ULF/ELF electromagnetic fields generated along the sea floor interface by a straight current source of infinite length. Radio Sci. **21**, 409–420, 1986

Knight, J.H., Raiche, A.P.: Transient electromagnetic calculations using the Gaver-Stehfest algorithm. Geophysics **47**, 47–50, 1982

Koski, R.A., Normark, W.R., Morton, J.L.: Massive sulfide deposits on the southern Juan de Fuca ridge: results of investigations in the USGS study area, 980-83. Marine Mining **5**, 147–164, 1985

Luke, Y.L.: Integrals of Bessel functions. New York: McGraw-Hill Book Co. 1962

Malahoff, A.: A comparison of the massive submarine polymetallic sulfides of the Galapagos Rift with some continental deposits. Marine Tech. oc. Jour **16**, 39–45, 1982

Normark, W.R., Morton, J.C., Koski, R.A., Clague, D.A., Delaney, J.R.: Active hydrothermal vents and sulfide deposits on the southern Juan de Fuca ridge. Geology **11**, 158–163, 1983

Parker, R.L.: The Frechet derivative for the one-dimensional electromagnetic induction problem. Geophys. J.R. Astron. Soc. **49**, 543–547, 1977

Rona, P.A.: Hydrothermal mineralization at slow-spreading centers: Red Sea, Atlantic Ocean, and Indian Ocean. Marine Mining **5**, 117–146, 1985

Stehfest, H.: Algorithm 368, numerical inversion of Laplace transforms. Commun. ACM **13**, 47–49, 1970

Tivey, M.K., Delaney, J.R.: Sulfide deposits from the Endeavour segment of the Juan de Fuca ridge. Marine Mining **6**, 165–180, 1985

Wait, J.R.: The fields of a line source of current over a stratified conductor. Appl. Sci. Res. **B3**, 279–292, 1953

Wait, J.R.: Theory of magnetotelluric fields. J. Res. NBS. Rad. Prop., 66D **5**, 509–541, 1962

Wolfgram, P.A., Edwards, R.N., Law, L.K., Bone, M.N.: Polymetallic sulfide exploration on the deep sea floor: the feasibility of the Mini-Moses technique. Geophysics **51**, 1808–1818, 1986

Received September 27, 1986; Revised March 9, 1987
Accepted March 10, 1987